IOPscience iopscience.iop.org

Home Search Collections Journals About Contact us My IOPscience

Analysis of the Hall effect in $TlGaTe_2$ single crystals

This article has been downloaded from IOPscience. Please scroll down to see the full text article.

2009 J. Phys.: Condens. Matter 21 235802

(http://iopscience.iop.org/0953-8984/21/23/235802)

View the table of contents for this issue, or go to the journal homepage for more

Download details:
IP Address: 129.252.86.83
The article was downloaded on 29/05/2010 at 20:08

Please note that terms and conditions apply.

J. Phys.: Condens. Matter **21** (2009) 235802 (5pp) doi:10.1088/0953-8984/21/23/235802

Analysis of the Hall effect in $TlGaTe_2$ single crystals

A F Qasrawi[1,2,4] **and N M Gasanly**[3]

[1] Group of Physics, Faculty of Engineering, Atilim University, 06836 Ankara, Turkey
[2] Department of Physics, Arab–American University, Jenin, West Bank, Palestine
[3] Department of Physics, Middle East Technical University, 06531 Ankara, Turkey

E-mail: aqasrawi@atilim.edu.tr

Received 20 February 2009, in final form 10 April 2009
Published 15 May 2009
Online at stacks.iop.org/JPhysCM/21/235802

Abstract
The electrical resistivity and Hall coefficient of p-type $TlGaTe_2$ crystals were measured in the temperature range of 110–320 K. The electrical resistivity, charge carrier density and Hall mobility data for the crystals have been analyzed by means of existing theories and models to determine the extrinsic energy levels, the carrier effective mass, the donor and acceptor concentrations and the dominant scattering mechanism in the crystal as well. The analysis of the temperature-dependent electrical resistivity recorded parallel and perpendicular to the crystal's axis (c-axis) reflected the existence of energy levels located at 0.26 and at 0.20 eV, respectively. The difference of these two energy levels is due to crystal anisotropy. The energy level at 0.26 eV was found to represent an acceptor level, as confirmed from Hall data analysis. The temperature dependence of the carrier density was analyzed by using the single-donor–single-acceptor model. The latter analysis revealed the carrier effective mass and the acceptor and donor concentrations as $0.73m_0$, 4.10×10^{17} cm^{-3} and 1.20×10^{17} cm^{-3}, respectively. The Hall mobility of $TlGaTe_2$ is found to be limited by the scattering of hole–acoustic phonon interactions. The calculated theoretical mobility fits to the experimental one under the condition that the acoustic deformation potential is 11.0 eV, which is the energy position of the top of valence band maximum that is formed by the Te 5s states.

1. Introduction

Recently, much attention has been devoted to systems that behave as if they had less than three spatial dimensions. Such kinds of materials are known as quasi-one/two-dimensional solids or chain/layered materials. $TlGaSe_2$, $TlGaS_2$ and $TlInS_2$ crystals belong to the quasi-two-dimensional solid group (layered crystals) and $TlInSe_2$, $TlInTe_2$ and $TlGaTe_2$ are in the quasi-one-dimensional solid group, in which the chains are constructed parallel to the c-axis. These characteristics limit the crystal physical properties. Most of the physical properties like the structural, electrical, optical and thermal properties of these crystals have been investigated and reported [1–13]. Some of the reported interesting features were the visible range photosensitivity, the second-harmonic generation and the high birefringence, along with a wide transparency range of 0.5–14 μm that makes the $TlGaSe_2$ crystals—for example—suitable for optoelectronic applications [8, 9]. In addition, the $TlInSe_2$ compound exhibits, in its electrical behavior, many nonlinear effects, such as S-type current–voltage characteristics, switching and memory effects [10].

Similarly to its partners, $TlGaTe_2$ crystal exhibits switching phenomena and negative differential resistance effects [14, 15] which allow it to play an important role in technological applications such as memory devices. Such properties make the $TlGaTe_2$ crystal attractive for researchers. As examples, the thermal expansion and isothermal compressibility [16] and the band structure and permittivity [17] of the crystal have been studied. The main purpose of this work was to study and discuss some more physical properties of the compound $TlGaTe_2$. In particular, the physical interpretation of the Hall properties and the single-donor–single-acceptor model analysis of the temperature-dependent carrier density, in addition to the analysis of the Hall mobility, will be reported.

[4] Author to whom any correspondence should be addressed.

 © 2009 IOP Publishing Ltd Printed in the UK

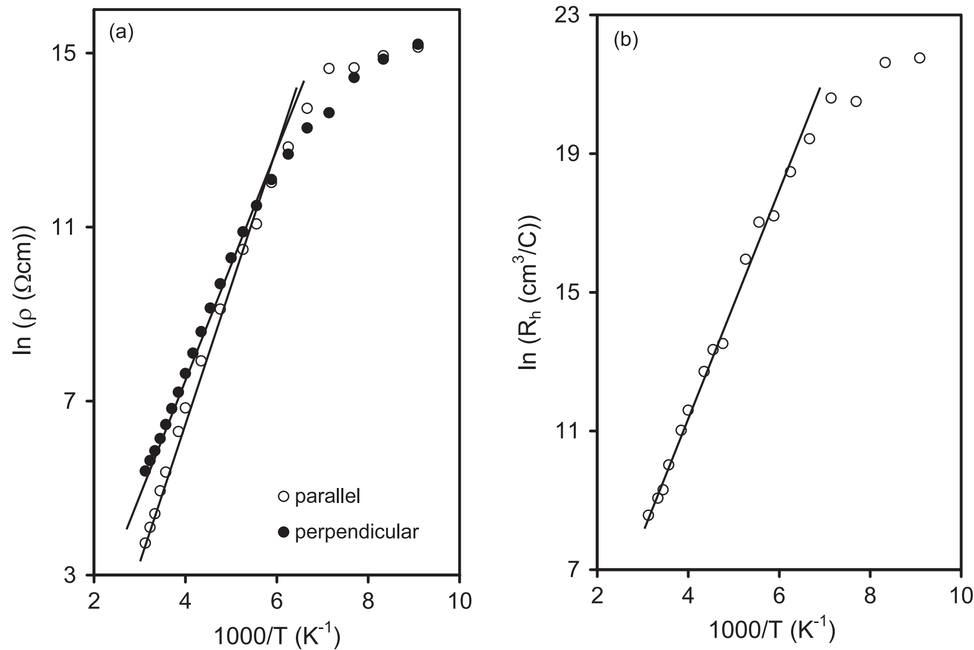

Figure 1. (a) The ln (ρ)–T^{-1} variation for $TlGaTe_2$ crystal. (b) The ln (R_h)–T^{-1} variation for $TlGaTe_2$ crystal.

2. Experimental details

$TlGaTe_2$ polycrystals were synthesized from high purity elements (at least 99.999%) taken in stoichiometric proportions. Single crystals of $TlGaTe_2$ were grown by the Bridgman method in evacuated (10^{-5} Torr) silica tubes with a tip at the bottom. The ampoule was moved in a vertical furnace through a thermal gradient of 30 °C cm^{-1}, between the temperatures of 775 and 425 °C, at a rate of 1.0 mm h^{-1}. The resulting ingots (gray in color) showed good optical quality and the cleaved mirror-like surfaces contained the chains parallel to the crystal c-axis extending along the [001] direction. The x-ray diffraction patterns show that these crystals have tetragonal structure with the lattice parameters $a = 0.8432$ and $c = 0.6863$ nm. The resulting single crystals were not subjected to any additional annealing. Typical dimensions of Hall bar-type samples were $15 \times 3 \times 0.2$ mm^3. For reliable electrical measurements, the electrical contacts were made by painting high purity silver paste using suitable masks. The ohmic nature of the contacts was confirmed by the I–V characteristic, which is found to be linear and independent of the reversal current for low applied voltages. The temperature-dependent dark electrical resistivity and Hall coefficient measurements were carried out in the temperature range 110–320 K in an automated closed-cycle Lakeshore cryogenic system. The temperature-dependent Hall effect measurements were recorded at a magnetic field ranging from 0.1 to 1.4 T.

3. Results and discussion

Accurate dark electrical resistivity (ρ) and Hall coefficient (R_h) measurements on $TlGaTe_2$ crystals were possible in the temperature range of 110–320 K. The sign of the Hall coefficient indicated that the crystals exhibit p-type conduction. The measured temperature-dependent electrical resistivity and Hall coefficient are illustrated in figures 1(a) and (b), respectively. During the Hall coefficient measurements, the current was applied parallel to the chains (c-axis), the magnetic field was applied along the direction perpendicular to the c-axis and the Hall voltage was recorded along the third perpendicular direction (standard Hall bar geometry). Thus, the values of all the recorded Hall effect data can be regarded as being perpendicular to the c-axis. The electrical resistivity measurements were carried out parallel ($\rho_\parallel$) and perpendicular ($\rho_\perp$) to the c-axis, respectively. Measurements of R_h along the c-axis were not possible due to the instrumental limitations in our laboratory. Figure 1(a) reflects the values of the electrical resistivity being recorded along and perpendicular to the chain (c-axis). Figures 1(a) and (b) display the sharp increases in the $\rho_\parallel$, $\rho_\perp$, and R_h values with decreasing temperature at two different rates above and below 160 K. In particular, $\rho_\parallel$, $\rho_\perp$, and R_h increased from 41.9 and 219.2 Ω cm, and 5.3×10^3 cm^3 C^{-1} at 320 K to 3.8×10^6 and 4.0×10^6 Ω cm, and 2.8×10^9 cm^3 C^{-1} at 110 K, respectively. The related room temperature carrier concentration and Hall mobility are found to be 1.4×10^{15} cm^{-3} and 105.0 cm^2 V^{-1} s^{-1}. Although the values of the electrical resistivity agree, the hole concentration and mobility values differ from those reported for the p-type $TlGaTe_2$ crystals: electrical resistivity, carrier density and Hall mobility values of 29.5 Ω cm, 4.3×10^{13} cm^{-3} and 4932 cm^2 V^{-1} s^{-1}, respectively [1]. The mobility value obtained in the present study is consistent with that reported as 96 cm^2 V^{-1} s^{-1} for $TlGaTe_2$ crystals [18]. The value of the electrical resistivity anisotropy may be attributed to the high concentration of the stacking faults due to weak inter-chain bonding [19] and/or the high

anisotropy of the direction-dependent effective masses in the crystal [20].

The measured $\rho(T)$ and $R_h(T)$ data can be represented by the following formulae:

$$\rho(T) = \rho_0 \exp\left(\frac{E_\rho}{kT}\right), \quad (1)$$

and

$$R_h(T) = R_{h0} \exp\left(\frac{E_{R_h}}{kT}\right), \quad \text{respectively.} \quad (2)$$

In the above equations, ρ_0 and R_{h0} are the pre-exponential factors of the related equations, E_ρ and E_{R_h} are the resistivity and Hall coefficient activation energies, respectively. Typical best fits for the experimental data are illustrated by the solid lines in figures 1(a) and (b). The values of $E_{\rho\parallel} = 0.258$ eV, $E_{\rho\perp} = 0.203$ eV, and $E_{R_h} = 0.267$ eV were determined from the slopes of these lines in the temperature range of 160–320 K. The calculated $E_{\rho\parallel}$ and E_{R_h} energy values are very close to each other, indicating that they relate to the same energy level, which on average may be regarded as 0.263 eV. Below 160 K, the $\rho(T)$–T and $R_h(T)$–T variations do not follow equations (1) and (2), predicting that another current transport mechanism may have become more dominant. That region of data (150–110 K) is insufficient for deriving any physical information. It is also important to recall that the contribution of the temperature dependence of the Hall mobility to the temperature dependence of the electrical resistivity and Hall coefficient is apparent through the relation $\mu(T) = R_h(T)/\rho(T)$. In other words, the variation of the Hall mobility and free carrier density with temperature lead to the temperature dependence of electrical resistivity as apparent in equation (1).

The values of the resistivity and Hall coefficient activation energies, being 0.203, 0.258 and ~0.267 eV, are comparable to those calculated from the current–voltage characteristics as 0.22 eV for $TlGaTe_2$ crystals [15]. They also agree well with those reported by Nagat *et al* [1] as 0.25 eV in the extrinsic conductivity region. The existence of this energy level in the band gap of the crystal may be due to structural defects such as Tl, Ga or/and Te vacancies and stacking faults created during the crystal growth process.

It is worth noting that the fitting procedure was carried out by a special high convergence minimization program that makes use of regression and residual sums of squares (R^2), the coefficient of determination and residual mean squares statistical analysis. The errors in the data were evaluated to be 3–13%. Typical best fits for the experimental data are illustrated in figure 1. All the calculated slopes were restricted to give a residual sum of squares $R^2 > 0.995$.

Figure 2 presents the behavior of the carrier concentration, $p(T)$, as a function of the reciprocal temperature for $TlGaTe_2$ crystals. The carrier concentration was calculated from the Hall coefficient by assuming a Hall factor of unity. As can be seen in figure 2, $p(T)$ drastically falls with decreasing temperature. The temperature dependence of the carrier

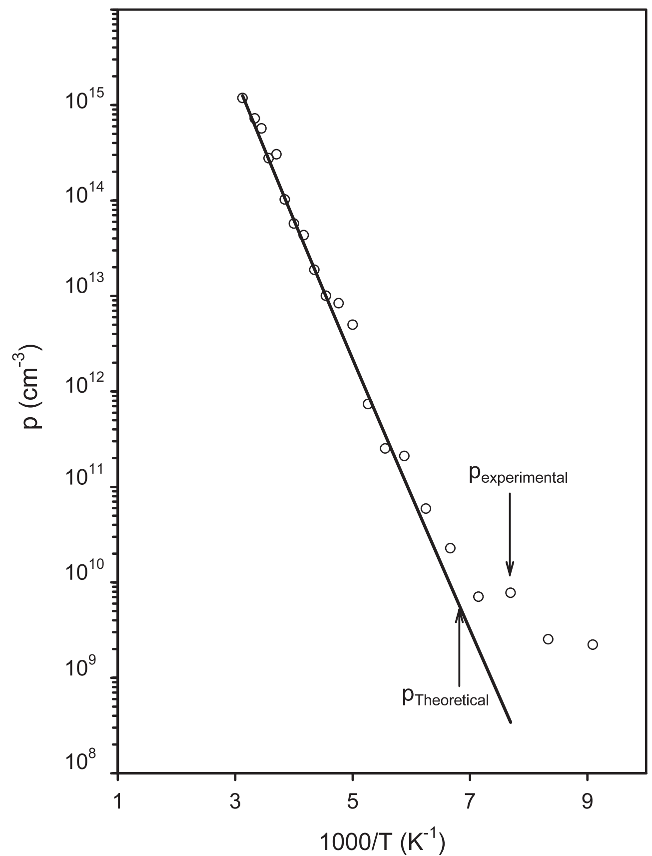

Figure 2. Variation of ln(p) versus T^{-1}. The solid line represents the fit according to equation (3).

concentration is analyzed by using the single-donor–single-acceptor model, in which the dependence of the carrier concentration on temperature is given by [21]

$$p = \{2(N_a - N_d)\}\left\{1 + \frac{N_d}{\beta N_v}\exp(E_a/kT) + \left[\left(1 + \frac{N_d}{\beta N_v}\exp(E_a/kT)\right)^2 + \frac{4(N_a - N_d)}{\beta N_v} \times \exp(E_a/kT)\right]^{1/2}\right\}^{-1} \quad (3)$$

where β is the degeneracy factor, $N_v = 4.83 \times 10^{15}(m_h^* T)^{3/2}$ (cm^{-3}) is the effective density of states of the valence band, N_a and N_d are the acceptor and donor impurity concentrations present in the crystal and E_a is the acceptor energy level from the top of the valence band. By substituting the degeneracy factor $\beta = 2$, and $E_a = 0.26$ eV, which is the value of the acceptor ionization energy calculated from equations (1) and (2), a computer numerical analysis was handled, using equation (3). The best fitting curve for the experimental data, obtained from the temperature-dependent Hall effect measurements, is represented by the solid line in figure 2. As a result of this fitting procedure, data regressions provided the determinations of the hole effective mass (m_h^*) and the acceptor and donor concentrations as $0.73m_0$, 4.1×10^{17} cm^{-3} and 1.2×10^{17} cm^{-3}, respectively. The acceptor–donor concentration difference ($N_a - N_d$) was found to be

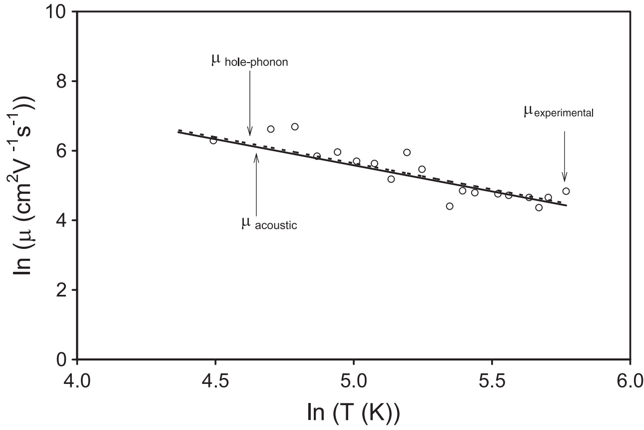

Figure 3. Plot of $\ln(\mu)$–$\ln(T)$ for $TlGaTe_2$ crystal. The dashed and solid lines represent the fits according to equations (4) and (6), respectively.

2.9×10^{17} cm^{-3}. The degree of compensation for $TlGaTe_2$ crystal was obtained as 0.7.

The experimental data for Hall mobility as a function of temperature are illustrated in figure 3. The mobility increases with decreasing temperature. The slope of the logarithmic plot of μ–T, was found to be ~ -1.8. This value is close to the drift mobility temperature dependence value (-1.5) indicating that thermal lattice scattering is dominant in the crystals.

Following our previous works on $TlGaS_2$, $TlInS_2$, $TlGaSe_2$ and $Tl_2InGaSe_4$ crystals [22, 23], we have tried to fit the experimental mobility assuming the dominance of hole–optical phonon short-range interaction scattering and/or hole–acoustic phonon interaction scattering.

The temperature dependence of Hall mobility of the hole–optical phonon short-range interaction mobility is given as [22]

$$\mu_{hp} = \frac{e\hbar\sqrt{\hbar\omega}}{3\sqrt{\pi}m_h^* g^2 (kT)^{3/2}}. \qquad (4)$$

Here, g^2 is the hole–optical phonon coupling constant.

The above relation is achieved using the hole–optical phonon short-range interaction in three dimensions for the optical phonon energy, $\hbar\omega$, being less than kT. The experimental Hall mobility data may be reproduced by equation (4) if $g^2 = 0.08$ and if $\hbar\omega = hc\nu = 0.012$ eV (valid above 140 K) are used. Here, $\nu = 97$ cm^{-1} is the frequency of the longitudinal optical mode obtained through IR measurements on $TlGaTe_2$ crystals [7]. The result obtained by this method is shown as a dashed line in figure 3.

The acoustic phonon scattering mobility is given by the relation [23]

$$\mu_{ac} = 3.17 \times 10^{-5} \frac{du^2}{(m_h^*)^{5/2} E_{ac}^2 T^{3/2}}, \quad cm^2\ V^{-1}\ s^{-1} \qquad (5)$$

where d is the density in $g\ cm^{-3}$, E_{ac} is the deformation potential in eV for acoustic phonons, and u is the average sound velocity, which can be estimated using the formula

$$u = \frac{k\theta_D}{\hbar}\left(\frac{V}{6\pi^2}\right)^{1/3} cm\ s^{-1}. \qquad (6)$$

Here θ_D is the Debye temperature estimated using Lindemann's melting rule and V is the average atomic volume. In computing the acoustic phonon scattering mobility, the values of d and V were calculated as 7.24 $g\ cm^{-3}$ and 4.88×10^{-22} cm^3, respectively, using the x-ray results (reported in section 2 of this paper) for the $TlGaTe_2$ crystal. θ_D was estimated as 128 K for a melting temperature of 1046 K.

When the above experimentally determined parameters were used to calculate the theoretical acoustic phonon scattering mobility (see equation (5)), the acoustic deformation potential, which provides the best fit to the experimental data in figure 3, was used as $E_{ac} = 11.0$ eV. This value is reported to represent the lowest energy position of the top of the valence band maximum that is formed by the Te 5s states [17]. The consistency between the experimentally determined and theoretically evaluated acoustic phonon scattering mobility data, plotted as a solid line, is displayed in figure 3.

It is worth noting that while estimating the theoretical value of the acoustic mobility no assumptions were used. All the parameters used were experimentally determined. On the other hand, the hole–optical phonon coupling constant, being 0.08, is very low as compared to those found for similar semiconductors like $TlInS_2$ ($g^2 = 0.64$), $TlGaS_2$ ($g^2 = 0.21$) and $TlGaSe_2$ ($g^2 = 0.17$) crystals [22]. These values of g^2 usually relate to weak hole–optical phonon interaction and moderate anisotropy. The g^2 values for pure metals, semiconductors and superconductors are reported to be $\sim$0.12–0.66, 0.15–0.90 and 0.40–1.48, respectively [25]. The low value of g^2 indicates rather weak interactions and means that the possibility of the scattering by hole–optical phonon short-range interactions is less dominant as compared to that for acoustic phonons. Thus, the experimental Hall mobility can be assumed to be limited by the scattering of hole–acoustic phonon interactions only.

Unfortunately, very few articles that discuss the temperature-dependent electrical conductivity and Hall mobility of $TlGaTe_2$ crystals have been previously published [1, 26]. The authors studied the electrical resistivity and Hall mobility in the temperature regions of 170–420 K [1] and 250–475 K [26]. They have shown that the crystal exhibits intrinsic character at high temperatures with a thermal band gap of $\sim$0.82 eV. The studies revealed extrinsic p-type conduction at low temperatures (below 274 K). The authors of [1] have evaluated an impurity level of 0.21 eV. They have also described the mobility behavior as being abnormal and obeying the laws $\mu \propto T^{4.4}$ and $\mu \propto T^{-3.6}$ in the intrinsic and extrinsic regions, respectively. They have attributed this abnormal behavior to the high density of stoichiometric vacancies and creation of defects in the crystal. The authors did not analyze the carrier concentration to obtain information about the carrier effective mass and acceptor and donor concentrations as well. Nor they were able to give a physical meaning for the mobility behavior. Their results are very different from what we have reported here. In our study we were not able to observe the intrinsic character because our measurements did not cover the high temperature region (the facility is not available in our laboratory). We believe that the difference between our results and those reported in [1] could be due to the methods

of growth of the crystals and the measuring techniques. For example, recording the Hall mobility at unstable temperatures (fast temperature increase with high heating rate) usually leads to high temperature dependence of the mobility. The μ–T dependence reported here was recorded at magnetic field values of 0.1–1.4 T in 0.1 T steps for each sample, and the behavior was the same for all applied magnetic fields.

Within the scope of the above reported results, one can observe significant differences in the properties of $TlGaTe_2$ as compared to $TlGaSe_2$ and $TlGaS_2$ [22–24]. In particular, $TlGaTe_2$ crystal exhibits lower resistivity ($\rho_{TlGaTe_2} = 82.2$, $\rho_{TlGaSe_2} = 1.7 \times 10^4$, $\rho_{TlGaS_2} = 1.1 \times 10^6 (\Omega\ \mathrm{cm})$), higher carrier concentration ($p_{TlGaTe_2} = 7.2 \times 10^{14}$, $p_{TlGaSe_2} = 5.9 \times 10^{12}$, $p_{TlGaS_2} = 1.0 \times 10^{11}$ (cm^{-3})) and higher Hall mobility ($\mu_{TlGaTe_2} = 105.0$, $\mu_{TlGaSe_2} = 62.0$, $\mu_{TlGaS_2} = 59.4$ ($\mathrm{cm^2\ V^{-1}\ s^{-1}}$)) at room temperature, higher hole effective mass ($m^*_{TlGaTe_2} = 0.73m_0$, $m^*_{TlGaSe_2} = 0.52m_0$, $m^*_{TlGaS_2} = 0.36m_0$) and weaker hole/electron–phonon interactions ($g^2_{TlGaTe_2} = 0.08$, $g^2_{TlGaSe_2} = 0.17$, $g^2_{TlGaS_2} = 0.21$) in addition to a complete change in the scattering mechanism from hole–optical phonon short-range interactions for $TlGaS_2$ and $TlGaSe_2$ to hole–acoustic phonon interactions for $TlGaTe_2$. The above data give an indication of significant systematic change in the electrical parameters of the III–VI semiconductors upon replacing S, Se and Te atoms (all three elements relate to the same group (VI) in the periodic table). The filling orbits for these elements are $3P^4$, $4P^4$, $5P^4$, respectively.

4. Conclusions

The dark electrical resistivity and Hall mobility measurements in the temperature range of 110–320 K for $TlGaTe_2$ layered crystals revealed that the crystals exhibit p-type conductivity. Measurements of the electrical resistivity parallel and perpendicular to the c-axis reflected the existence of crystal anisotropy. The electrical resistivity and Hall coefficient are observed to increase while the carrier concentration decreases with decreasing temperature. The temperature dependence of the carrier concentration was analyzed using the single-donor–single-acceptor model. The data analysis revealed hole effective masses of $0.73m_0$, a degree of compensation of 0.7 and an acceptor–donor concentration difference of $2.9 \times 10^{17}\ \mathrm{cm}^{-3}$. The temperature-dependent electrical resistivity analysis suggests the existence of impurity levels located at ~0.26 eV and at ~0.20 eV in the energy gap of the crystals obtained parallel and perpendicular to the c-axis, respectively. The Hall mobility data were analyzed in accordance with the existing theories of thermal lattice scattering and found to be limited by the hole–acoustic phonon scattering. Since anisotropic Hall effect measurements were not possible due to laboratory instrumental limitations, the role of anisotropy in determining the above parameters was not obtained.

References

[1] Nagat A T, Gamal G A and Hussein S A 1991 *Cryst. Res. Technol.* **26** 19

[2] Hanias M, Anagnostopoulos A, Kambas K and Spyridelis J 1992 *Mater. Res. Bull.* **27** 25

[3] El-Nahass M M, Sallam M M, Rahman S A and Ibrahim E M 2006 *Solid State Sci.* **8** 488

[4] Abutalybov G I, Abdullaeva S G and Zeinalov N M 1982 *Sov. Phys.—Semicond.* **16** 1348

[5] Grivickas V, Bikbajevas V and Grivickas P 2006 *Phys. Status Solidi* b **243** R31

[6] Qasrawi A F and Gasanly N M 2004 *Semicond. Sci. Technol.* **19** 505

[7] Gasanly N M, Goncharov A F, Dzhavadov B M, Melnik N N, Tagirov V I and Vinogradov E A 1980 *Phys. Status Solidi* b **97** 367

[8] Ibragimov T D and Aslanov I I 2002 *Solid State Commun.* **123** 339

[9] Allakhverdiev K R 1999 *Solid State Commun.* **111** 253

[10] Hanias M, Anagnostopoulos A, Kambas K and Spyridelis J 1991 *Phys. Rev.* B **43** 4135

[11] Abay B, Guder H S, Efeoglu H and Yogurtcu Y K 2001 *J. Phys. Chem. Solids* **62** 747

[12] Abay B, Efeoglu H, Yogurtcu Y K and Alieva M 2001 *Semicond. Sci. Technol.* **16** 745

[13] Qasrawi A F and Gasanly N M 2008 *J. Phys.: Condens. Matter* **20** 155204

[14] Nassary M N, Hussein S A and Nagat A T 1994 *Cryst. Res. Technol.* **29** 869

[15] Hanias M P and Anagnostopoulos A 1993 *Phys. Rev.* B **47** 4261

[16] Kurbanov M M 2005 *Inorg. Mater.* **41** 1277

[17] Godzhaev E M, Orudzhev G S and Kafarova D M 2004 *Phys. Status Solidi* **46** 833

[18] Guseinov G D, Mooser E, Kerimova E M, Gamidov R S, Alekseev I V and Ismailov M Z 1969 *Phys. Status Solidi* **34** 33

[19] Parlak M, Ercelebi C, Gunal I, Ozkan H and Gasanly N M 1996 *Cryst. Res. Technol.* **31** 673

[20] Riede V, Neumann H and Sobotta H 1981 *Solid State Commun.* **38** 71

[21] Blackmore J S 1962 *Semiconductor Statistics* (London: Pergamon) p 135

[22] Qasrawi A F and Gasanly N M 2006 *Cryst. Res. Technol.* **41** 174

[23] Qasrawi A F and Gasanly N M 2008 *J. Phys.: Condens. Matter* **20** 155204

[24] Guseinov G D, Abdullayev G B, Bidzinova S M, Seidov F M, Ismailov M Z and Pashayev A M 1970 *Phys. Lett.* A **33** 421

[25] Poole C P 1999 *Handbook of Superconductivity* (New York: Academic) chapter 9, Sec. G pp 478–83

[26] Abdel-Rahman M 1998 *Indian J. Pure Appl. Phys.* **36** 533